


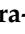



Article

Thermal Performance, Microstructure Analysis and Strength Characterisation of Agro-Waste Reinforced Soil Materials

Monica C. M. Parlato ^{1,*}, Simona M. C. Porto ¹, Carmen Galán-Marín ², Carlos Alberto Rivera-Gómez ², Massimo Cuomo ³ and Francesco Nocera ³

- ¹ Department of Agriculture, Food and Environment, University of Catania, Building and Land Engineering Section (Di3A), Via S. Sofia 100, 95123 Catania, Italy; simona.porto@unict.it
- ² Departamento de Construcciones Arquitectónicas 1, Escuela Técnica Superior de Arquitectura, Universidad de Sevilla, Avda. de Reina Mercedes, 2, 41012 Seville, Spain; cgalan@us.es (C.G.-M.); crivera@us.es (C.A.R.-G.)
- ³ Department of Civil Engineering and Architecture (DICAR), University of Catania, V.le Andrea Doria 6, 95125 Catania, Italy; francesco.nocera@unict.it (F.N.)
- * Correspondence: monica.parlato@unict.it

Abstract: The use of raw-earth materials reinforced by natural fibres, i.e., livestock waste in the form of greasy wool, represents an eco-friendly alternative for a variety of construction applications. This proposal is based on the analysis of unfired adobe blocks stabilised with wool fibres for use as both structural and non-structural building materials. The influence of fibre length on the thermophysical and mechanical properties of the tested material was investigated. The thermal conductivity coefficient (λ) of raw-earth samples was assessed by following three different test setting procedures ($T = 20\text{ }^{\circ}\text{C}$, and HR at 30%, 50%, and 70%), with the aim to evaluate the effects of different fibre lengths in the raw-earth mix. Samples reinforced by fibres 20 mm in length exhibited the lowest thermal conductivity coefficient ($\lambda = 0.719\text{ W/mK}$) obtained by a test reproducing typical indoor conditions within the Mediterranean area, i.e., $T = 20\text{ }^{\circ}\text{C}$, and HR 50%. The best mechanical performance was exhibited by samples reinforced by fibres 40 mm in length, with a flexural and compression strength of 0.88 MPa and 2.97 MPa, respectively. The microstructure of these biocomposites was also examined with a scanning electron microscope (SEM) and an energy dispersive X-ray (EDX) to qualitatively evaluate the variation of thermal and mechanical properties due to the different adhesion among the fibres and the soil. The experimental data show good efficiency and a significant improvement in the behaviour of these materials compared to the control samples. The evaluation of the results, with the length of the fibres being the only variable of the analysed samples, allowed for the identification of the mix suitable for the best mechanical and thermal performances, depending on the final use of the material.



Citation: Parlato, M.C.M.; Porto, S.M.C.; Galán-Marín, C.; Rivera-Gómez, C.A.; Cuomo, M.; Nocera, F. Thermal Performance, Microstructure Analysis and Strength Characterisation of Agro-Waste Reinforced Soil Materials. *Sustainability* **2023**, *15*, 11543. <https://doi.org/10.3390/su151511543>

Academic Editors: Gianluca Scaccianoce, Giorgia Peri and Laura Cirrincione

Received: 28 June 2023
Revised: 14 July 2023
Accepted: 16 July 2023
Published: 26 July 2023



Copyright: © 2023 by the authors. Licensee MDPI, Basel, Switzerland. This article is an open access article distributed under the terms and conditions of the Creative Commons Attribution (CC BY) license (<https://creativecommons.org/licenses/by/4.0/>).

Keywords: raw-earth materials; agro-waste; thermal performance; SEM

1. Introduction

Nowadays, the use of alternative eco-friendly materials, recyclable and renewable with a low footprint impact, could contribute to the development of a more sustainable building sector by reducing its impact. Furthermore, the conversion to a green building approach is also increasing the interest in biocomposite materials; a biocomposite is a material composed of a matrix combined with one or more distinct constituents, generally reinforcement fibres. These two or more components are mixed together to produce a new material suitable for physical and mechanical performances [1]. In this context, the interest in earthen building materials for new constructions or the renovation of existing ones, and the contemporary re-use of wastes, could be of relevant importance in the circular economy framework, which is one of the main requirements for the European Green Deal, (EGD) [2]. There are several advantages that come from the use of raw-earth-based materials, all related to a significant decrease in environmental pollution and CO₂ emission

(e.g., the release of carbon dioxide into the atmosphere is 80% less than fired bricks). Raw-earth-based building components, if realised without chemical additives (i.e., through only physical and mechanical stabilisation), can be easily recycled to produce new earthen products at the end of their use life, or they can be disaggregated and returned to the natural environment with negligible environmental impact [3,4]. Furthermore, if raw earth is extracted and worked directly at the building site, logistical and transportation costs, and the associated environmental pollution, are reduced. Raw-earth-based building components are important for their ability to increase air quality and for their thermal regulating properties in indoor environments. Thanks to their thermal mass, they are suitable for humidity absorption/desorption rate and heat storage power; the result of their use is the balance and control of indoor acoustic and temperature variation improving thermal comfort [1]. This ecological material contributes significantly to increasing thermal comfort and the healthy aspects of construction by balancing the indoor climate [5]. If relative humidity (RH) is more than 40–60% (i.e., the optimal zone for human well-being [6]), bacteria and moulds can grow, affecting thermal performance and indoor air quality. Shukla et al. evaluated the energy consumption for the construction and maintenance of an adobe house. They demonstrated that adobe houses save about 370 GJ of energy and 101 tons of CO₂ emissions per year compared to traditional constructions [7]. In the literature, the dry thermal conductivity value of raw-earth components is usually reported between 0.8 and 0.9 W/m K, and specific weight ranges between 1850 and 2210 kg/m³ [8]. Galan et al., in their study calculated for a stabilised soil panel, made in proportions by weight of 76.75% clay, 20% water, 3% alginate, and 0.25% sheep wool fibre, a thermal transmittance (U-value) of 0.78 W/mK [9]. Munñiz et al. [10] investigated the thermal properties of adobe bricks reinforced with paper and pulp waste and found an average thermal conductivity of 0.861 [W/mK] for the control sample and a λ of 0.608 [W/mK] for a sample with consisting of 20% pulp. Worldwide, it is estimated that about 998 million tons of agricultural waste are produced yearly [11]. In addition, a significant increase in agricultural waste, valued from 5% to 10%, is caused by the intensive farming system and the extreme use of chemical fertilisers [12]. The unplanned reuse of these kinds of waste is a big issue for environmental pollution, such as soil contamination, air pollution, and degradation of the rural landscape. Lately, the valorisation of agricultural waste has become an important step for environmental protection, energy saving, and sustainable development, which has been studied by Karade [13], Raut et al. [14], Madurwar et al. [15], and Kazmi et al. [16]. The use of organic waste is becoming a passive technique for energy saving within the building sector [17]. Several studies assessed the use of agricultural waste (AW) as natural additives within unfired earth materials [18–20]. The focus of these works is mainly on agro-waste fibre recovery and utilisation (e.g., wheat straw fibres, straw fibres, and Hibiscus cannabinus fibres) [21]. Researchers are working to investigate the potential use of natural fibres as reinforcement composites instead of synthetic ones (e.g., glass fibre, polymeric fibres), to improve mechanical properties, shrinkage rate, and ductility of the composite [22,23]. This increasing attention to natural fibres is not only due to their properties, but also to their recyclability, low cost, high availability, and low production carbon footprint (i.e., the total amount of greenhouse gases produced expressed in equivalent tons of carbon dioxide (CO₂)). Furthermore, the addition of fibres increases thermophysical properties, thanks to their low thermal conductivity and light weight. Several works have investigated the fibres' effects on raw-earth materials from a mechanical point of view. Fewer studies have analysed the thermal performance variations deriving from the addition of fibres, and most of them are related to vegetable fibres. Giroudon et al. investigated the effects of barley and lavender straw in unfired earth bricks by varying fibre concentration (i.e., 3%, 6% by mass) [24].

They found that by increasing the percentage of fibres, thermal conductivity decreases; the lowest values measured were 0.28 W/mK for samples with 6% lavender straw and 0.15 W/mK for samples with 6% barley straw. Jannat et al., in their review, reported the

influences of agro-fibre waste (e.g., banana fibre, rice husk, sisal fibre, kenaf fibre, henequen fibre, jute, pig hair, and sheep wool) on the thermal properties of unfired earth blocks [25].

Also, in this case, the thermal efficiency of the unfired earth samples increased with the addition of fibre waste. Thermal conductivity decreases thanks to the low thermal conductivity of fibres and due to the higher porosity in the mix deriving from their presence, which could affect mechanical strength. Moreover, the addition of fibres decreases the density, and the lower the density, the lower the thermal conductivity [26]. Bogas et al. [27] and Oti et al. [28] also found that density, void volume, and thermal conductivity are correlated. Benkhadda et al. [29] proved that the thermal conductivity in unfired clay bricks decreases with the addition of sheep wool into the mixture.

As they stated, unfired clay bricks reinforced with sheep wool are suitable to improve the thermal efficiency of housing envelopment. In this study, with the aim of adding information about an eco-friendly material suitable for passive design strategies (i.e., methods and devices incorporated into the building to improve heat transfer and storage, increasing its energy efficiency [30,31], thermal tests were carried out on raw-earth samples reinforced with low-quality sheep wool fibre (SWF).

Strazzeri et al. investigated the thermal effectiveness of using Spinifex fibres as bulk insulation for rammed earth materials. They found that the inclusion of Spinifex fibres improves the material's thermal performance. Table 1 illustrates the thermal conductivity of rammed earth construction [32].

Table 1. Values of thermal conductivity of rammed earth construction.

Material	Density [kg/m ³]	Thermal Conductivity [W/mK]
NRE (natural rammed earth)	1400–2200	1–1.4
SRE (stabilised rammed earth)	2000–2100	0.8–1
SRL (stabilised rammed limestone)	2100	1.1
SRL + bulk insulation	1800–1500	0.8–0.5
CEBs (compressed earth blocks) + coconut fibres	1700–1500	0.9–0.7
CEBs + Alfa fibres	3000–2500	1.5–1.17

NRE = natural rammed earth, SRE = stabilised rammed earth, SRL = stabilised rammed limestone, CEB = compressed earth blocks.

As the mechanical and thermal behaviours of the raw-earth-based building components are sensitive to both soil composition and fibre addition, SWF length varied to evaluate the optimal mix design. Moreover, in this research, a scanning electron microscope (SEM) and energy-dispersive X-ray (EDX) were used to explore the microscopic structural variations in raw-earth samples. The aim was to examine the correlation between the mechanical strength and thermal capacity measured through the interaction between the fibre and matrix bond. These interactions control the load transfer between the fibres and the matrix, the chemical bonds, the secondary interaction forces (van der Waals, acid/base etc.), and the mechanical interconnecting [33,34]. A comprehensive analysis was carried out to investigate the microstructural interface among fibres and matrix bonds, an interface that could affect both the thermal capacity of the composites and the mechanical strength. Experimental results on the physical features of raw-earth-based materials were reported. Samples were realised by using the same soil mix design and fibre percentage (0.25% in weight) varying only the fibre length (from 10 mm fibres to 40 mm fibres). Four different repetitions were performed for each mix design. The length of the SWF was changed to evaluate the best mix design. According to the results obtained, the reinforcement by fibres is essential to improve the thermal performance of the bio-compound and the ductility of the material.

This paper is structured as follows: the materials and methods section describes the materials used to prepare the samples, the samples' composition, the thermal test, and a description of the SEM and EDX investigations. Then, the results section shows the

investigation results. In the discussion section, the obtained data are further analysed and discussed, finally ending with the conclusion section.

2. Materials and Methods

2.1. Materials and Samples Preparation

The soil utilised in this study is a mix created by combining clay and pyroclastic sand with kaolinite soil and was dubbed “Terra di Florida” (FS).

FS is soil extracted in Syracuse (South Italy, Sicily) that is distinguished by a simple extraction technique and a low transport cost. The Atterberg Limits of FS [31] are shown in Table 2. The clay contained in FS is kaolinite ($\text{Al}_2\text{Si}_2\text{O}_5(\text{OH})_4$) a silicate mineral with one tetrahedral sheet of silica (SiO_4) linked through oxygen atoms to one octahedral sheet of alumina (AlO_6) octahedra. With the aim to improve the mechanical behaviour of FS, its particle size distribution was modified through the addition of clay [3]. This resulted in an FS modified (FS^{M}) with the rate of 58% FS soil and 42% clay, by weight. Clay addition increases cohesion and plasticity and reduces water absorption by improving erosion resistance to wind and capillary waterproofing.

Table 2. Atterberg Limit of Florida Soil.

Physical Characteristics	[%]
Liquid Limit (LL)	47.30
Plastic Limit (PL)	30.68
Plasticity Index (PI)	16.62

Then, to improve mechanical resistance and to prevent shrinkage and cracking issues, FS^{M} was mixed with pyroclastic sand typical of the Etna volcano area called ‘*azolo*’. Figure 1 shows the grading of the final mix (FS^{M}). Particle size distribution was determined through a sieve analysis carried out in accordance with the ASTM D7928—17 requirements, by using material dried in an oven at 100 °C.

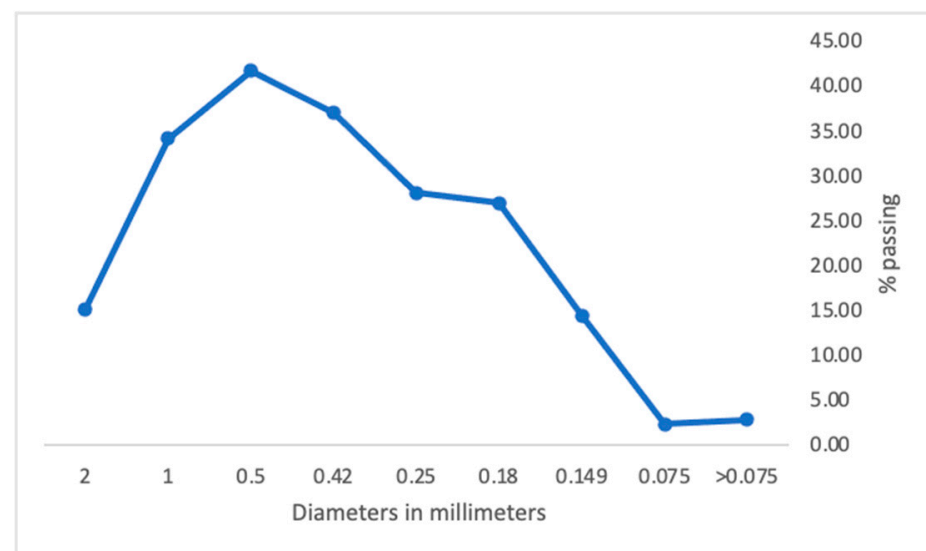


Figure 1. Particle size of the final mix (including sand).

‘*Azolo*’ is generated by the crushing of glassy materials produced by the quick cooling of magma on the surface of lava. It is generally employed in the concrete industry to improve the mechanical resistance of the composite [35].

Considering the sample preparation, the mix used for the realisation of them was prepared by adding to FS^{M} pyroclastic sand and water (Table 3). This soil mix was selected by authors in a previous study [4].

Table 3. Mix design used in this work.

FS ^M (%)	Florida Soil 58 %		Sand (%)	Water (%)
	Clay 42%			
45			35	20

The preparation of the samples started with the addition of fibres to the homogeneous soil mix, i.e., FS^M and sand. All specimen preparation and compaction processes have been executed manually. The compaction energy was not monitored because only manual compaction was performed; nevertheless, the manufacturing water content of the mix was controlled during the process. For each formwork, the same amount of mix was cast to obtain the design density of 1800 kgm⁻³.

SWFs were slowly and carefully added to the clay soil to reduce the formation of fibre bundles. In the end, once the fibres were fully incorporated into the mixes, water was added in four steps, manually stirring between each step. The samples were cast in consecutive layers and compacted by hand applying sufficient pressure. Samples were prepared with the same soil mix by changing only the length of the fibres and keeping the fibre percentage constant (Table 4). For each combination, four repetitions have been tested. Sheep wool fibres, 10 mm, 20 mm, and 40 mm in length, were randomly distributed in the soil mix at a rate of 0.25% by weight. The samples were manually compacted and cast in 100 mm × 100 mm steel cubic moulds. After casting, samples were cured for at least 28 days in the laboratory with an average temperature of 20 °C and relative humidity of 60%.

Table 4. ID and mix design of samples.

Number of Samples	Number of Repetitions	Test Purpose	Specimen's Type
16	4	Thermal Conductivity	Cube (100 × 100 × 100)
	Wool [%]	SWF Length [mm]	Mix
	-	-	ID 0
	0.25	10	ID 10–25
	0.25	20	ID 20–25
	0.25	40	ID 40–25

Figure 2 is showing the specimens used to carry out experimental trials.

**Figure 2.** Samples used to carry out thermal tests.

The mechanical characteristics of the mix design used in this work and shown in Table 4 were deeply investigated by authors in a previous study [36]. Mechanical tests have been carried out in accordance with European standards (EN 1015-11:2019) [37] to evaluate flexural and compressive strengths. The results shown in Table 5 include average values of flexural and compressive tests, dry density, and linear shrinkage rate.

Table 5. Average mechanical values of the reinforced mix [38].

Linear Shrinkage Rate [%]		Dry Density [kg/m ³]		Average Compression Strength [MPa]		Average Flexural Strength [MPa]		Wt [%]	Fibre Length [mm]	Mix
μ	σ	μ	σ	μ	σ	μ	σ			
0.25	6.25	0.05	1960.0	0.43	3.05	0.18	0.89	-	-	ID 0
0.36	4.35	0.03	1904.3	0.29	3.14	0.16	0.68	0.25	10	ID 10–25
0.34	4.75	0.08	1890.0	0.35	3.13	0.17	0.78	0.25	20	ID 20–25
0.33	4.84	0.03	1844.5	0.35	2.97	0.19	0.88	0.25	40	ID 40–25

As appears by analysing the data shown in Table 4, mix ID 10–25 and ID 20–25 obtained the best values for compression strength, 3.14 [MPa] and 3.13 [MPa], respectively; the best flexural strengths were obtained by the nonfibrous mix with 0.89 [MPa] (mix ID 0), and by ID 40–25 with 0.88 [MPa]. The different failure mode among fibrous and nonfibrous samples was also assessed. As determined by several authors, the addition of the fibres in the mix determines a change in failure mode from fragile to ductile [36].

As underlined in the two typical load-displacement curves represented in Figure 3, samples realised without reinforcement fibre have a sudden drop in load because of the formation of unstable macroscopic cracks after the maximum load; on the contrary, reinforced samples registered a ductile failure mode with the two parts linked together even after failure.

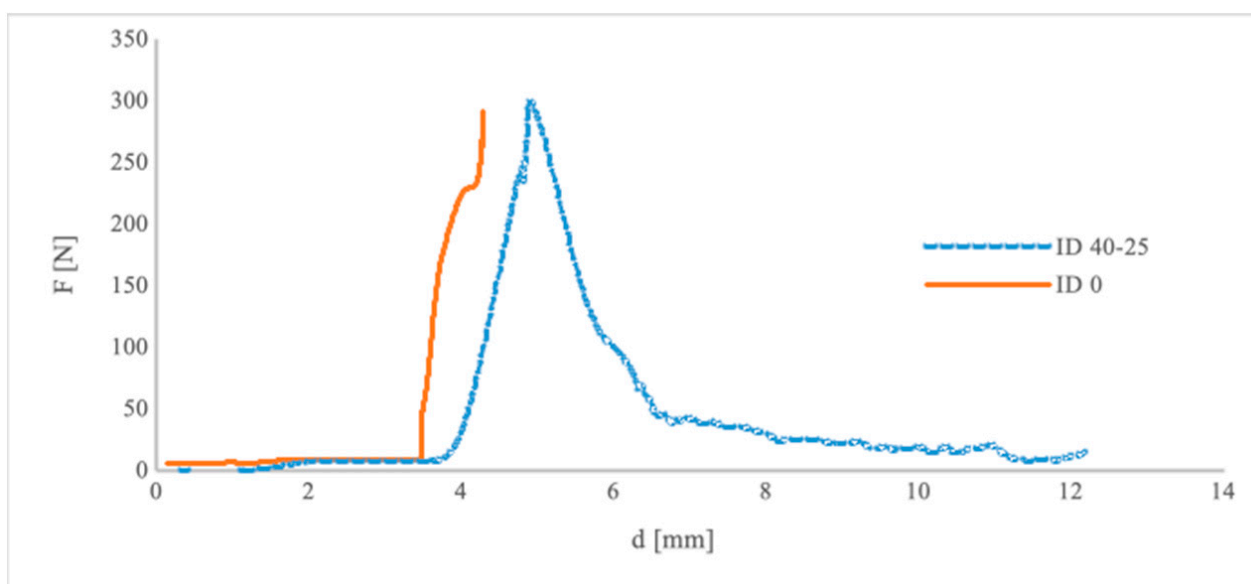
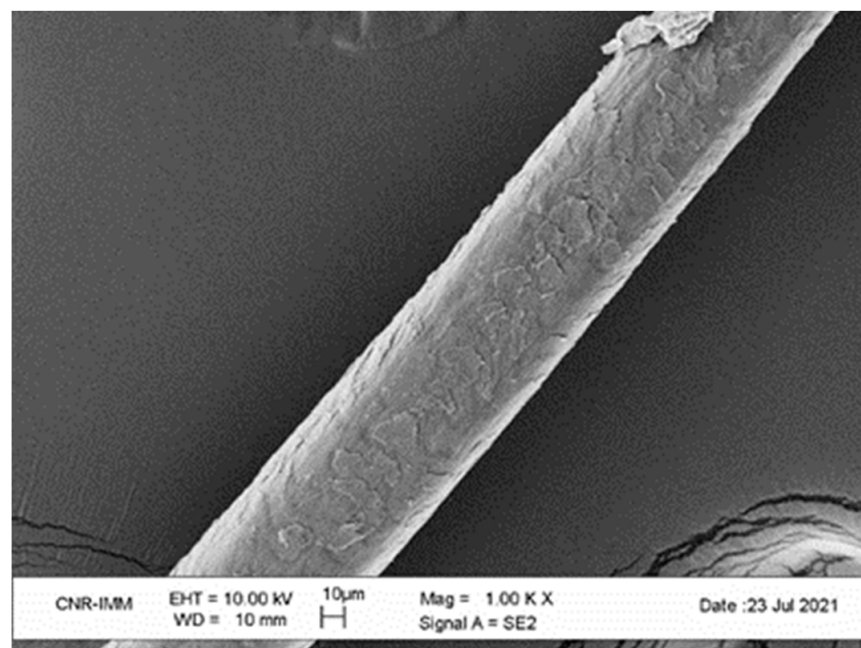


Figure 3. Load displacement curve of fibrous samples dotted line (SWF 0.25%, length 40 mm) and nonfibrous specimen continue the line.

The addition of wool increased the ability of the composite to support load even after the first crack and the ultimate strain leading to a ductile failure mode before the collapse. Parlato et al. [38] considered the energy absorbed by the fibrous and nonfibrous earthen material until the deflection at the final fracture. By assessing the fracture energy, measured

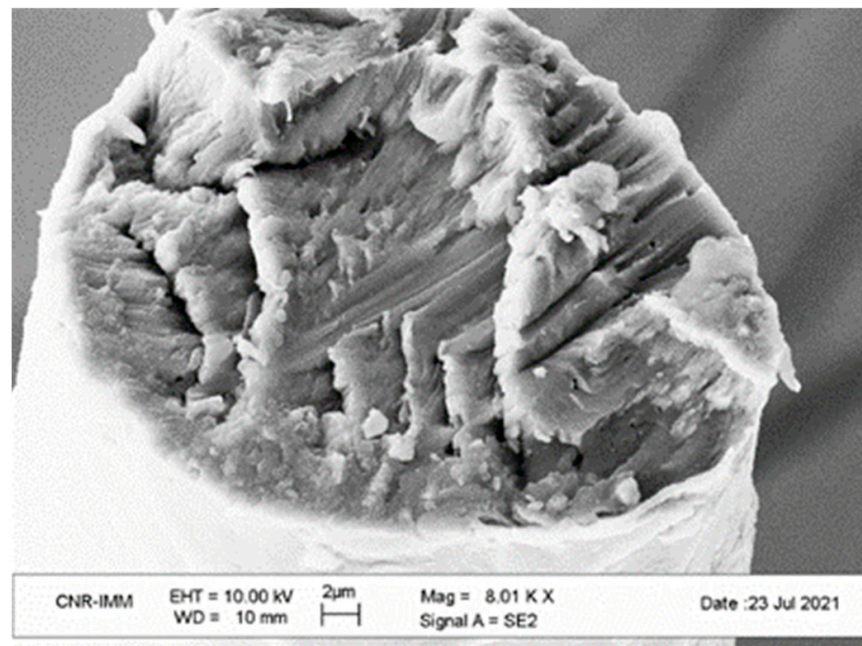
as the area under the load-displacement curve, the structural response of the material in terms of first-crack resistance, post-cracking performance, and energy absorption capability, has been evaluated. They obtained a mean value of fracture energy of 806.38 [N/mm] for the wool fibrous' sample; for the control sample, a sample without wool-reinforced fibres, the last displacement observed was equal to the peak displacement, so fracture energy could not be measured due to the quick load drop and the complete loss of residual strength after the peak load. In this work, raw wool, as a livestock waste material, has been integrated into raw-earth samples. The waste used is raw sheep wool, derived from the sheep breeder sector and belonging to the "Valle del Belice" species, which is highly widespread in Sicily. Sheep wool, among animal fibres, is appropriate for a variety of purposes in various disciplines and sectors, particularly to increase building thermal efficiency, due to its mechanical, chemical, and physical properties. Furthermore, when compared to standard thermal and acoustic insulation materials (such as polyurethane foam, polystyrene, glass wool, and rock wool), wool is more efficient while having a reduced carbon footprint. This wool is unsuitable for the textile industry because the fleece is of thick and medium-length fibres [39]. By current Regulations (EC Regulation 1069 (2009), EU Regulation 142 (2011)), wool is an animal by-product (ABPs) requiring specific procedures for handling, treatment and disposal, and transportation; this means high disposal costs for breeders. The valorisation of this ABP could contribute to decreasing environmental pollution by the reduction of a huge amount of waste by becoming an economic benefit for a breeder. In a previous study [40], a sample of this kind of wool constituting 180 fibres that were randomly selected, was deeply characterised by the authors. With the aim to assess the behaviours of this raw sheep wool and its potential use as a reinforcement fibre in raw-earth materials, its physical and mechanical performances have been assessed. The obtained results encouraged the use of SWF as reinforcing material: 137.31 [MPa] is the average tensile strength found, and elongation at break was determined to be 42.00%.

Figure 4a,b, shows a scanning electron microscopy (SEM) analysis of the wool fibre surface and transversal section. SEM analysis was carried out at "Torre Biologica" of the University of Catania.



(a)

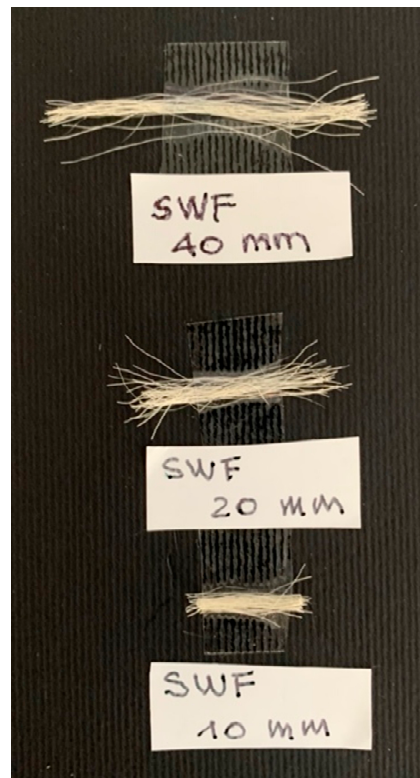
Figure 4. Cont.



(b)

Figure 4. SEM analysis of sheep wool fibre surface and transversal section (a,b).

In Figure 5, a and b show the three fibre lengths used in this work, e.g., 10 mm, 20 mm, and 40 mm, and their introduction into the soil mix.



(a)



(b)

Figure 5. SWF of 10 mm, 20 mm, and 40 mm length and SWF introduction into the mix (a,b).

2.2. Methods Used

2.2.1. Thermal Test

The ASTM D5334-14 Standard Methods [41] were used to evaluate the thermal conductivity of the raw-earth samples. Thermal conductivity was measured with a needle probe (TLS-100, THERMTEST Portable System, Hanwell, NB, Canada) with a large length-to-diameter ratio to approximate the circumstances of an indefinitely long, infinitely thin heating source. The theory of this approach is based on the solution of the line heat source situated within an infinite, isotropic, and homogeneous medium of thermal diffusivity (D [m^2/s]); the heat flows from the source in accordance with the Fourier equation. The needle is heated during the test, and the temperature change is recorded. Carslaw and Jaeger [42] found an analytic solution for the transient-line heat source generated by the probe. They assumed that the heat is produced from time $t = 0$ at a constant rate q per unit length of the probe; by considering that the increment of temperature (ΔT) is linearly related to time variation ($\ln t$) and that the expanding radial field around the probe is small with respect to the diffusivity (D), their approximate equation is followed [43]:

Where q is the heat input rate [W/m], k is the thermal conductivity [$\text{W}/(\text{m K})$], t is the heating time [s], and c is a constant. The plot of this equation gives a function of time on a semi-log graph. By considering the linear portion of this curve, times t_1 and t_2 are selected and the corresponding temperatures T_1 and T_2 are read. Finally, by considering the slope S of the function (1), thermal conductivity k can be evaluated:

$$\Delta T \approx \frac{q}{4\pi k} \ln t \quad (1)$$

$$\Delta T \approx \frac{q}{4\pi k} \ln t + c \quad 0 < t < t_h \quad (2)$$

$$k = \frac{q}{4\pi S} \quad (3)$$

where:

$$S = \frac{T_2 - T_1}{\ln t_2 - \ln t_1} \quad (4)$$

So, the test consists of heating the needle inserted into the specimen by measuring temperature. Before beginning the thermal test, the needle probe was calibrated by comparing the experimental determination of a standard material's thermal conductivity to its known value.

The calibration factor, G , was calculated as follows:

$$G = \frac{\lambda_{material}}{\lambda_{measured}} \quad (5)$$

where:

$\lambda_{material}$ is the known thermal conductivity of the calibration material, i.e., the needle probe, and:

$\lambda_{measured}$ is the thermal conductivity of the specimen measured with the thermal needle probe apparatus.

All measurements with the thermal needle probe were multiplied by G before being reported. The sensor needle was completely inserted into the specimen, which was previously drilled at low speed and cleared of dust. To minimise any contact resistance between the sensor and specimen, the needle was completely covered by a thermal paste with $\lambda > 4 \text{ m}^{-1} \text{ K}^{-1}$. Later, a known current and voltage were applied to the probe to raise the temperature. Temperature rises and decreases after the cessation of heating and the time that occurred during this phase were recorded. Thermal conductivity (λ) was obtained from the analysis of the temperature-time series data during the heating cycle. Thermal tests were performed on samples under a constant temperature of 20°C by varying the

relative humidity conditions. All samples before thermal measurements were kept inside a climatic cabinet in accordance with the following test setting:

First setting condition: 24 h at T 20 °C and RH 30%

Second setting condition: 24 h at T 20 °C and RH 50%

Third setting condition: 24 h at T 20 °C and RH 70%

Figure 6 shows an example of thermal conductivity measurements.



Figure 6. Thermal conductivity measurements.

2.2.2. SEM and EDX Analysis

This section aims to elucidate the variation in thermal and mechanical properties due to the different interphase soil-reinforcement void distributions caused by shrinkage. The samples were examined by scanning electron microscopy (SEM), using a JEOL JSM-6460LV microscope and by an energy-dispersive X-ray analyser (EDX). SEM and EDX are suitable tools for the study of the spatial relationships between the soil matrix and reinforcement fibres. These analytical tests were carried out in the CITIUS laboratory of the University of Seville (Seville, Spain). By performing SEM and EDX investigation, it is possible to evaluate the degree of bonding between the particles of soil and the natural fibres. This allows a better understanding of the micro-morphology of the natural fibres and their effect on the overall composite material structure.

3. Results

3.1. Thermal Conductivity

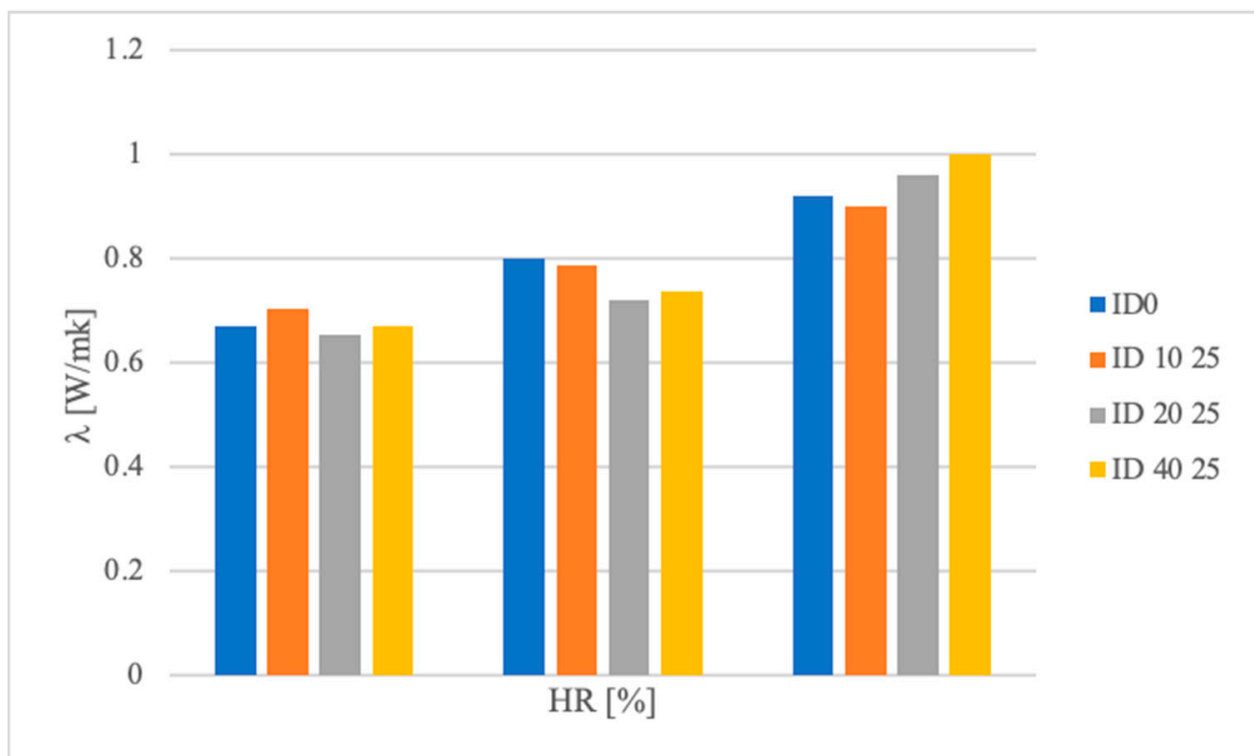
The thermal conductivity (λ) of raw-earth samples was assessed following three different setting conditions by changing the relative humidity percentage rate, as described in Section 2.2.1. Table 5 reports the average values of measured thermal conductivity. Results obtained by the thermal characterisation of the tested samples provide a data range for the thermal conductivity coefficient between 0.654 [W/mK] and 0.705 [W/mK] for the test carried out following the 1st test condition (HR 30%); between 0.719 [W/mK] and 0.801 [W/mK] under the 2nd test condition (HR 50%); and between 0.90 [W/mK] and 1.00 [W/mK] under the 3rd test condition (HR 70%). The soil displaying the best thermal properties corresponded to the mix ID 20–25, as shown by the results of the samples. The second test setting reproduced the typical ambient condition in a Mediterranean climate area. In this context, the worst values of conductivity were obtained by samples without fibre addition (ID 0, λ of 0.801 [W/mK]). On the contrary, samples made with mix ID 20–25, that is with a fibre length of 20 mm, exhibited a lower value of 0.654 [W/mK]. This mix was the best performer under the first set condition with $\lambda = 0.719$ [W/mK]. Under the third test condition, the best thermal conductivity of 0.90 [W/mK] was obtained by samples ID 10–25, with fibres 10 mm in length. Table 6 summarises the obtained thermal conductivity values.

Table 6. Thermal conductivity of raw-earth cube tested in this study.

λ [W/mK] T = 20° HR = 70%	λ [W/mK] T = 20° HR = 50%	λ [W/mK] T = 20° HR = 30%	ρ [g/cm ³]	Wool [%]	Wool Length [mm]	Mix ID
0.92	0.801	0.669	1.94	-	-	ID 0
0.90	0.787	0.705	1.90	0.25	10	ID 10–25
0.96	0.719	0.654	1.93	0.25	20	ID 20–25
1.00	0.736	0.670	1.89	0.25	40	ID 40–25

The effect of fibre length on the thermal behaviour of the composite in samples ID 40–25 can be observed. By increasing the length of the fibre in the composite, the thermal conductivity decreases until the threshold length of 40 mm where there is a trend reversal.

By considering the obtained results, it is possible to establish that the addition of fibres in the mix improves its thermal behaviours as already stated in the literature [22]; this is true except for tests performed under the extreme condition of HR 70%. In this case, samples with long fibres (40 mm) exhibited the worst result, with an average λ of 1.00 [W/mK]. The high hygroscopicity of earthen material and sheep wool fibres both have a considerable influence on thermal conductivity values in this scenario [44–47]. Thermal conductivity values of the highest quality were obtained in samples reinforced with short and medium fibres. This reduced conductivity observed in fibrous samples is attributable to the action of the fibres, which enhance porosity by lowering the material's density. The thermal conductivity values discovered are comparable to those published in the literature for similar materials [48–50]. Figure 7 shows in detail the variation of thermal conductivity for sample ID 0, ID 10 25, ID 20 25, and ID 40 25, by varying the HR percentage (30%, 50%, or 70%).

**Figure 7.** Variation of thermal conductivity by varying HR percentage (30%, 50%, and 70%).

The correlation between dry density and thermal conductivity has also been investigated, but a clear tendency has not been found. Only under the first setting condition, with an HR of 30%, did the R-value reach 0.42. The absence of a clear correlation between dry density and the thermal conductivity of raw material has already been demonstrated in the literature [51]. From the graph analyses, it appears that the fibres influence the thermo-physical behaviour of the samples. Thermal performance is a function of both fibre length and moisture content. The behaviour of the samples is similar for lengths between 20 and 40 mm while it is noted a change in thermo-physical behaviour with 10 mm fibre length. The benefits of the fibres are obtained up to values of 20 mm. To find the optimal ratio between the length of the fibres and the percentage of spaces occupied by them with the same % of wool required further investigation, as described in the following paragraph.

3.2. Microstructural Property Analysis

In this study, the boundary interphase soil reinforcement and void distribution have been investigated to establish a possible relationship with the thermal conductivity and mechanical strengths of the composite material investigated. Samples were examined by scanning electron microscopy (SEM), and different shrinkage degrees around the wool fibres were detected depending on the length of fibre added. The adhesion between the fibres and soils was mainly affected by the compression friction forces appearing on the surface of the reinforcing fibre due to the shrinkage of the soil [34].

During the cast and curing process, wool fibres suffer an important dimensional change caused by water absorption, moisture, and temperature variation. The water absorption produces an expansion of the fibres that initially pushes away the soil (at a microscopic level), and after the drying process, when the fibres lose the moisture and come back to their original dimensions, this phenomenon causes voids around the bonding between fibres and soil. For each fibre length (10 mm, 20 mm, 40 mm) three different repetitions were analysed. Figure 8 shows the samples used for SEM and EDX analysis. These samples were obtained by cutting the original samples (100 mm × 100 mm × 100 mm) in the middle section away from the edge. In order to be imaged using SEM, the specimen requests a conductive surface and has to be placed inside a high vacuum.

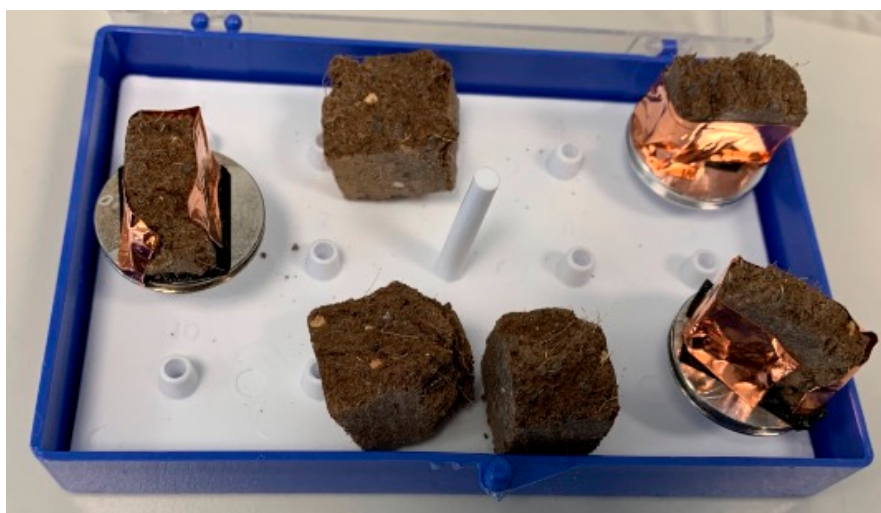


Figure 8. Samples used for SEM and EDX analyses.

As can be seen in Figures 9a,b–11a,b different shrinkage degrees around the wool fibre were detected depending on the length of fibre used.

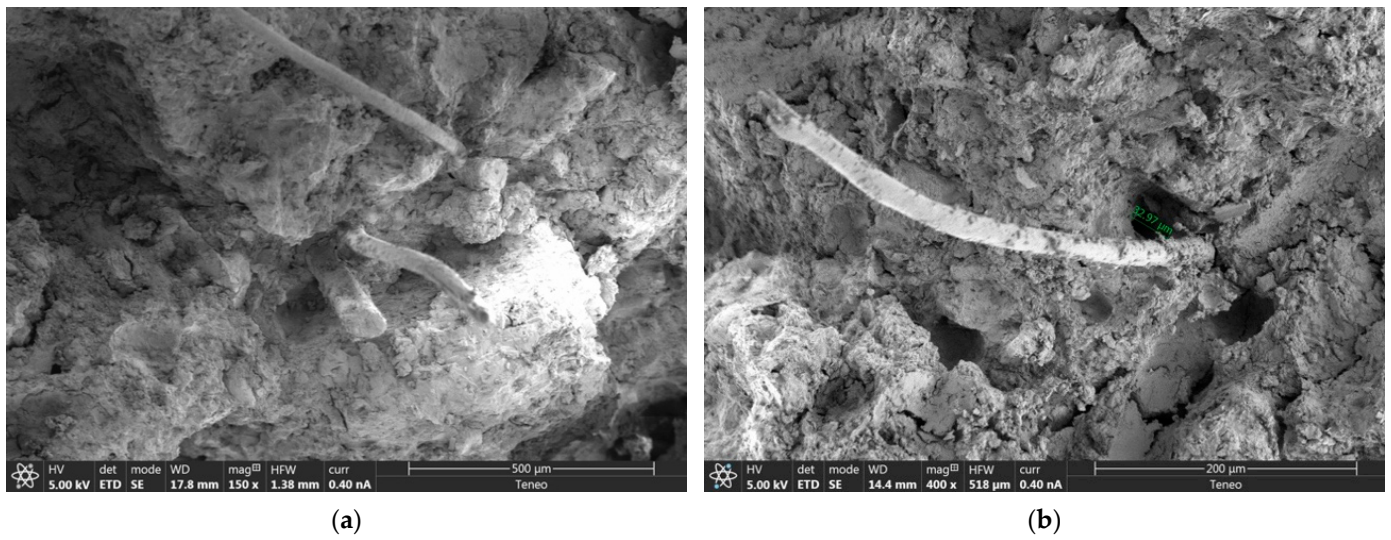


Figure 9. (a,b), SEM images of samples with fibres of 10 mm.

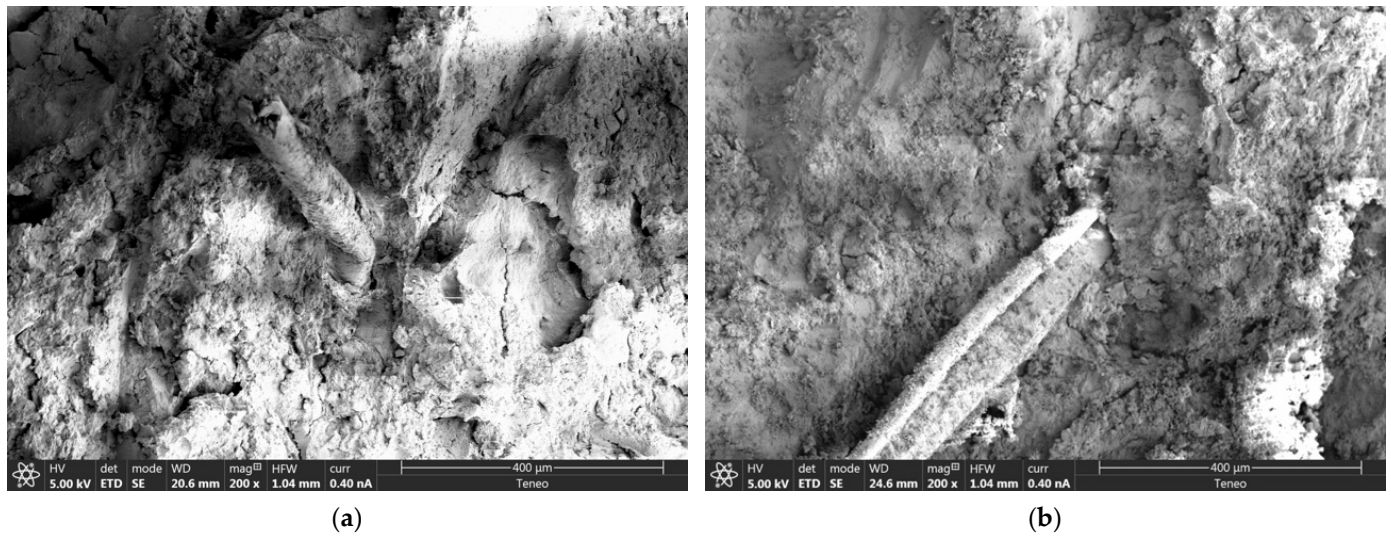


Figure 10. (a,b), SEM images of samples with fibres of 20 mm.

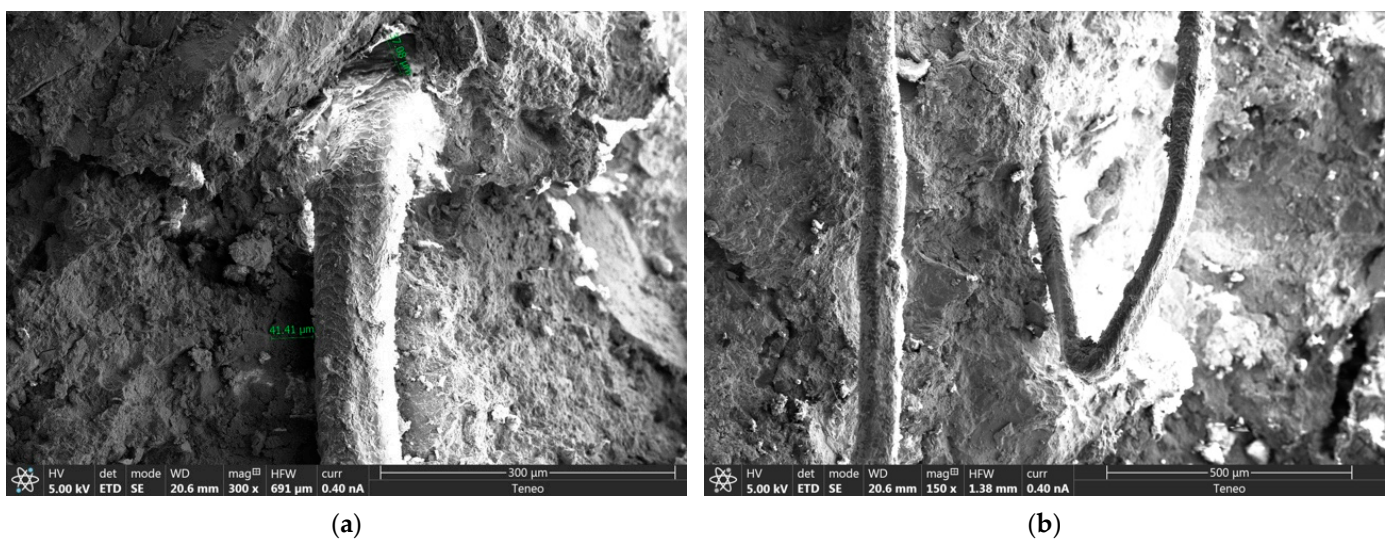


Figure 11. (a,b), SEM images of samples with fibres of 40 mm.

The soil retraction ranges were of a smaller margin in longer fibres samples ($\leq 41.40 \mu\text{m}$) and became more relevant in the case of 10 mm fibres giving a variation in the shrinkage measurements of these samples ranged between 0 and $59.90 \mu\text{m}$ (Table 7).

Table 7. Voids' radius measurements at the fibre–matrix interface.

	Shrinkage Range (μm)	Wool Length
1st	0–59.90	10 mm
2nd	0–49.33	20 mm
3rd	0–41.40	40 mm

Moreover, as illustrated in Figures 8a and 9b, mixes that contain shorter fibres tend to suffer from fibre bunching; clusters formed by 4 or 5 fibres appeared due to SEM analyses. The cause is the difficulty in producing samples for each of the employed fibre lengths; also, because the fibres are added by weight, the 10 mm fibres have four times the number of 40 mm fibres for the same fibre % (that is, the same weight). This phenomenon has a large impact on a little building component.

These clusters generate cracks inside the samples and give rise to lower flexural behaviour compared to samples with longer wool fibre. In fact, by comparing SEM exploration with flexural strengths results (Table 4) the higher values were reached by samples with longer fibres that do not exhibit cluster formation inside the matrix and by control samples, cast without fibres addition.

Then, the EDX test was performed to obtain information on the chemical composition of the mineralogical phases of the soils.

The EDX microanalyses were performed on a benchtop to quantify the chemical elements present in the soil. All samples were analysed under low vacuum using an 18 kV electron beam and were covered with a thin metallic film. Figure 12 shows the two portion analysed in the sample by SEM image and EDX analysis (spot 1 and spot 2).

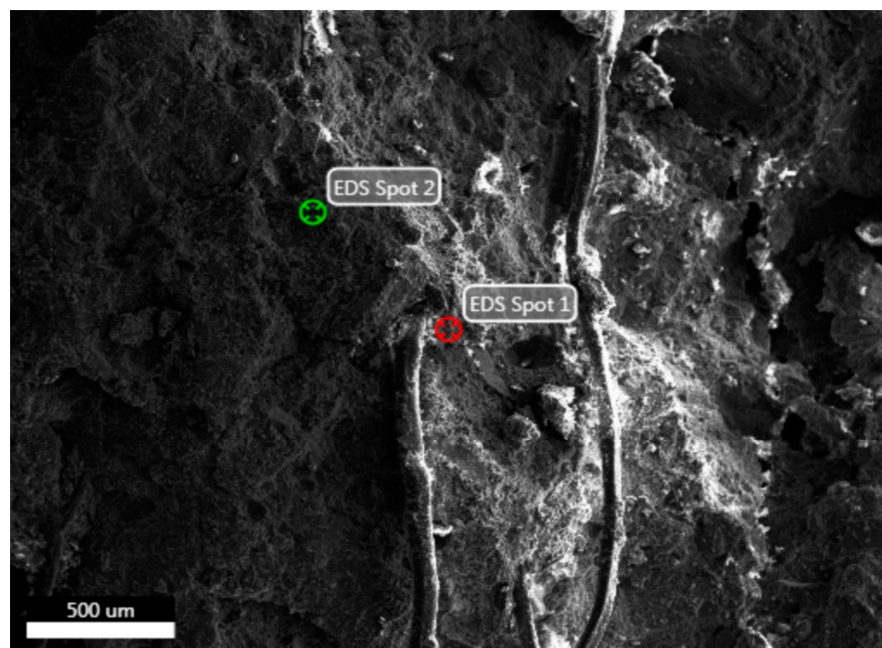


Figure 12. SEM image of EDX analysed spot.

The EDX test confirmed (Figures 13 and 14), by a semi-qualitative analysis, the chemical composition of the soils in the samples analysed (Tables 8 and 9).

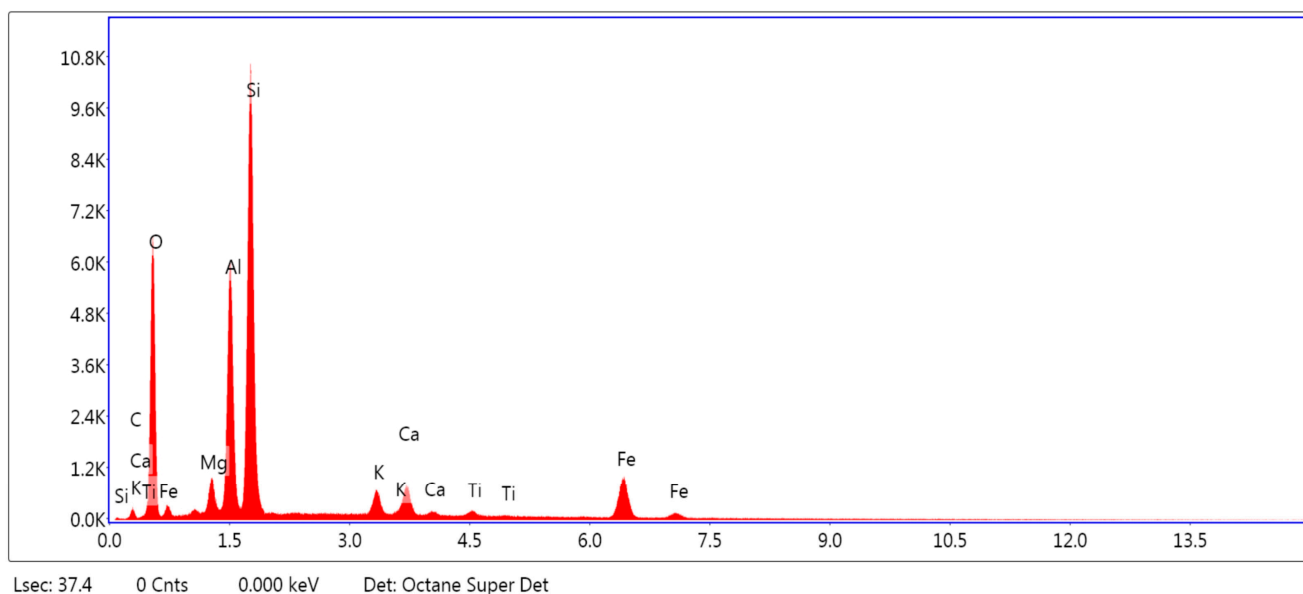


Figure 13. EDX spectra of a sample (close to fibre), spot 1.

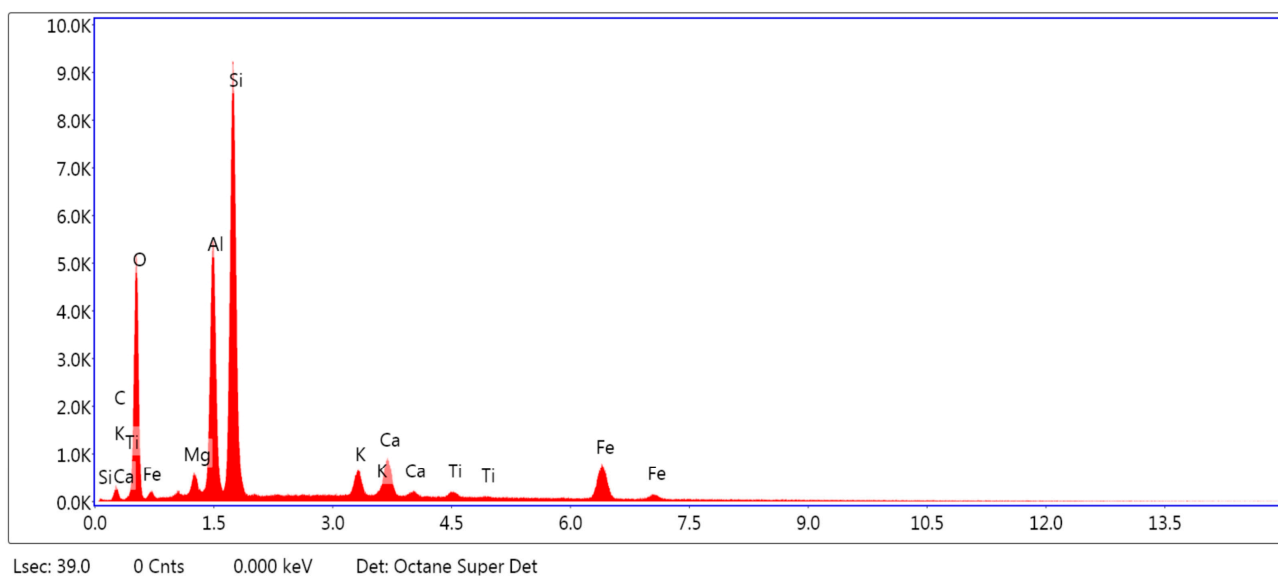


Figure 14. EDX spectra of a sample (mainly soil), spot 2.

Table 8. Chemical composition of the sample showed in Figure 12, spot 1.

Formula	Atomic %	Weight %	Element
CO ₂	3.21	1.73	C K
O	56.24	40.43	O K
MgO	1.76	1.93	MgK
Al ₂ O ₃	11.14	13.51	AlK
SiO ₂	19.67	24.83	SiK
K ₂ O	1.31	2.29	K K
CaO	1.86	3.36	CaK
TiO ₂	0.35	0.75	TiK
FeO	4.45	11.18	FeK

Table 9. Chemical composition of the sample showed in Figure 12, spot 2.

Formula	Atomic %	Weight %	Element
CO ₂	6.10	3.32	C K
O	54.05	39.21	O K
MgO	0.90	0.99	MgK
Al ₂ O ₃	11.38	13.93	AlK
SiO ₂	19.22	24.47	SiK
K ₂ O	1.46	2.59	K K
CaO	2.54	4.62	CaK
TiO ₂	0.41	0.89	TiK
FeO	3.94	9.98	FeK

Tables 8 and 9 report the chemical composition of the samples shown in Figure 12, spot 1 and spot 2. By analysing these two tables, the first concerning a spot with fibre addition and the second about a spot with mainly soil, no evident differences emerged in the chemical composition of the mineralogical phases of the soils. Despite the use of raw fibres, the chemical substances linked to the fibres do not enter into chemical interaction with the soil.

4. Discussion

This investigation analysed the effect of different fibre lengths on the physical and mechanical characteristics of biocomposites made from soil reinforced with wool fibres. The work has identified parameters involved in their mechanical and thermal performance to adapt these materials to the necessary technical and functional requirements. With the aim of understanding the variation of the mechanical and thermal properties of raw-earth material caused by the different interphase soil-reinforcement and void distributions, a scanning electron microscopy (SEM) technique was used.

The increase of strength properties in the composite fibre/soil mix mostly depends on the formation of fibre-matrix bonds. Lower flexural resistance values were obtained when shorter fibres were introduced to the mix. Conversely, specimens with long fibres exhibited higher strength, largely due to the absence of clusters inside the matrix and the minimum size of void detected. The longer fibres did not form bundles, resulting in a more homogeneous behaviour of the material.

Concerning the mechanical results, the compression strength is similar for the tested samples (ranging around 3 MPa). By considering flexural tests, the best result was achieved by sample ID 40 25. Moreover, the reinforced Mix ID 25 40 exhibited the lowest level of shrinkage.

The interpretation of the thermal tests must be conducted considering the porosity results.

The scanning electron microscopy (SEM) technique was used in this research in order to determine the specificities of the porosity and microstructure of the samples. On the micrographic images, at high magnification, a series of porous networks and micro-cracks, due to the drying process and voids around the wool fibres, were observed.

Further examination of the samples at the fibre–matrix interface implied variations in the radius measurements of these perimeter voids around the fibres. The difference may be due to the combination of the soil’s water retention owing to the cluster formation and the absorption–desorption processes of the wool fibres. These measurements could be established in different ranges, being between 0 and 41.40 µm for samples incorporating longer fibres, between 0 and 49.33 µm for samples incorporating 20 mm fibres, and between 0 and 59.90 for samples incorporating shorter fibres (Table 7).

Regarding the thermal conductivity, total pore area and average pore diameter are particularly significant sample features to be considered.

Thermal conductivity values obtained were as follows:

- First setting test ($T = 20\text{ }^{\circ}\text{C}$, HR = 30%) λ ranged between 0.654 [W/mK] and 0.705 [W/mK].
- Second test condition ($T = 20\text{ }^{\circ}\text{C}$, HR = 50%) λ ranged between 0.719 [W/mK] and 0.801 [W/mK].
- Third test condition ($T = 20\text{ }^{\circ}\text{C}$, HR = 70%) λ ranged between 0.688 [W/mK] and 0.770 [W/mK].

5. Conclusions

Sustainability and energy efficiency in the construction sector are focused on reducing primary energy consumption, lowering CO₂ emissions, and improving the ecological behaviours of conventional and non-traditional building materials. In particular, increasing the sustainability of buildings requires the use of alternative materials acquired through recycling waste, such as agricultural waste. Furthermore, the valorisation of locally accessible resources, such as agricultural waste, co-products, or by-products, and their application in the building sector is critical for long-term development, particularly in rural regions. This is an excellent method for reducing environmental impact and contributing to the achievement of a Nearly Zero Energy Building (NZEB).

This research investigated the mechanical and thermal properties of raw-earth construction components reinforced with animal fibres, namely sheep wool fibres, with the goal of generating an eco-friendly material that may help improve indoor microclimates. Investigations on the link cohesiveness between fibres and the matrix, which influences thermal and mechanical performances, were also conducted, with an emphasis on the impact of fibre length. SEM pictures were effective in determining the varied degrees of shrinkage around the fibres and matrix bond.

Based on the results illustrated above, we conclude the following:

- Short and medium fibre samples showed the best values of thermal conductivity, around 0.705 [W/mK].
- By analysing the SEM pictures and measuring the voids around the fibres, it was concluded that samples with longer fibres had smaller voids and no bundles. This is the reason for the high thermal conductivity measured. On the contrary, samples with shorter fibres exhibit bigger voids and bundles.
- These analyses are in accordance with measured thermal conductivity since a lower value of conductivity was obtained by samples with shorter fibre lengths where the bigger voids were detected.
- Control Sample ID 0, with the higher dry density, registered higher conductivity.
- The best performance was obtained with ID 20–25. In fact, this mix obtained low thermal conductivity, good compressive strength, and acceptable flexural strength.
- The addition of fibres to the mix determines the decrease in dry density from 1960.0 [kg/m³] to 1890.00 [kg/m³].
- The effects of fibre addition on the failure mode of samples improve the ductility of the material by changing the failure mode of samples.
- SWF addition causes a decrease in tensile strength, except for longer fibres where smaller voids were detected by SEM analyses; on the contrary, compressive strength is not particularly affected by fibre length.

Obviously, depending on the final usage of the material, the designer will select the best length of fibres to improve the thermal or mechanical properties of the composite. Longer fibres of 40 mm in length provide the optimum mechanical performance for structural materials; however, when thermal qualities are required, smaller fibres of 10- or 20-mm length must be used for the production process.

More research is needed to complete the picture of earthen construction composites reinforced with sheep wool fibres, including their hydrothermal characteristics, weather resistance, and durability.

Author Contributions: Conceptualisation, M.C.M.P., C.A.R.-G., C.G.-M. and F.N.; methodology, M.C., F.N. and C.A.R.-G.; software, M.C.M.P.; validation, C.A.R.-G., C.G.-M. and F.N.; formal analysis, M.C.M.P. and C.A.R.-G.; resources, C.G.-M. and C.A.R.-G.; data curation, M.C.; writing—original draft preparation, M.C.M.P., C.A.R.-G. and C.G.-M.; writing—review and editing, M.C.M.P., C.A.R.-G., C.G.-M. and F.N.; visualisation, S.M.C.P.; supervision, C.G.-M., C.A.R.-G., F.N. and M.C. All authors have read and agreed to the published version of the manuscript.

Funding: This research received no external funding.

Institutional Review Board Statement: Not applicable.

Informed Consent Statement: Not applicable.

Data Availability Statement: Not applicable.

Acknowledgments: This research study was carried out within a research project at the University of Catania: UPB: 5A722192127 (Piano per la ricerca 2016–2018-Task 2.3—“IT applications for innovation in the field of territorial and rural landscape planning”). The authors want to thank the CITIUS (Centro de Investigación, Tecnología e Innovación Universidad de Sevilla) for the access to the SEM and EDX tests and the support of the research group USE-TEP 206 SATH Sustainability in Architecture, Technology and Heritage (Universidad de Sevilla). The authors would also like to thank the “Laboratorio di Sostenibilità Energetica ed il controllo ambientale (SECA)”, University of Catania, for providing the measuring instruments.

Conflicts of Interest: The authors declare no conflict of interest.

References

- Fagone, M.; Kloft, H.; Loccarini, F.; Ranocchiali, G. Jute fabric as a reinforcement for rammed earth structures. *Compos. Part B Eng.* **2019**, *175*, 107064. [CrossRef]
- European Commission. The European Green Deal. *Eur. Comm.* **2019**, *53*, 24. [CrossRef]
- Achenza, M.; Sanna, U. *Il Manuale Tematico Della Terra Cruda*; DEI: Ivrea, Italy, 2009; Volume 1, p. 2. Available online: <https://hdl.handle.net/11584/63365> (accessed on 1 May 2023).
- Parlato, M.; Porto, S.M.; Cascone, G. Raw earth-based building materials: An investigation on mechanical properties of Florida soil-based adobes. *J. Agric. Eng.* **2021**, *52*. [CrossRef]
- Bouasria, M.; El Mendili, Y.; Benzaama, M.-H.; Pralong, V.; Bardeau, J.-F.; Hennequart, F. Valorisation of stranded *Laminaria digitata* seaweed as an insulating earth material. *Constr. Build. Mater.* **2021**, *308*, 125068. [CrossRef]
- Alsomo, T. Relative Humidity, RH (%), a Problem or Not in Swedish Buildings. *J. Environ. Prot.* **2019**, *10*, 1299–1316. [CrossRef]
- Shukla, A.; Tiwari, G.; Sodha, M. Embodied energy analysis of adobe house. *Renew. Energy* **2009**, *34*, 755–761. [CrossRef]
- Sabbà, M.F.; Tesoro, M.; Falcichio, C.; Foti, D. Rammed Earth with Straw Fibers and Earth Mortar: Mix Design and Mechanical Characteristics Determination. *Fibers* **2021**, *9*, 30. [CrossRef]
- Galán-Marín, C.; Martínez-Rocamora, A.; Solís-Guzmán, J.; Rivera-Gómez, C. Natural Stabilized Earth Panels versus Conventional Façade Systems. Economic and Environmental Impact Assessment. *Sustainability* **2018**, *10*, 1020. [CrossRef]
- Muñoz, P.; Letelier, V.; Muñoz, L.; Bustamante, M. Adobe bricks reinforced with paper & pulp wastes improving thermal and mechanical properties. *Constr. Build. Mater.* **2020**, *254*, 119314. [CrossRef]
- Bories, C.; Borredon, M.E.; Vedrenne, E.; Vilarem, G.; Agamuthu, P. Challenges and Opportunities in Agro-Waste Management: An Asian Perspective What Is AgroWaste? *J. Environ. Manag.* **2009**, *143*, 186–196. [CrossRef]
- Koul, B.; Yakoob, M.; Shah, M.P. Agricultural waste management strategies for environmental sustainability. *Environ. Res.* **2021**, *206*, 112285. [CrossRef]
- Karade, S. Cement-bonded composites from lignocellulosic wastes. *Constr. Build. Mater.* **2010**, *24*, 1323–1330. [CrossRef]
- Raut, S.; Ralegaonkar, R.; Mandavgane, S. Development of sustainable construction material using industrial and agricultural solid waste: A review of waste-create bricks. *Constr. Build. Mater.* **2011**, *25*, 4037–4042. [CrossRef]
- Madurwar, M.V.; Ralegaonkar, R.V.; Mandavgane, S.A. Application of agro-waste for sustainable construction materials: A review. *Constr. Build. Mater.* **2013**, *38*, 872–878. [CrossRef]
- Kazmi, S.M.S.; Munir, M.J.; Patnaikuni, I.; Wu, Y.-F.; Fawad, U. Thermal performance enhancement of eco-friendly bricks incorporating agro-wastes. *Energy Build.* **2018**, *158*, 1117–1129. [CrossRef]
- Hafez, F.S.; Sa’Di, B.; Safa-Gamal, M.; Taufiq-Yap, Y.; Alrifayy, M.; Seyedmahmoudian, M.; Stojcevski, A.; Horan, B.; Mekhilef, S. Energy Efficiency in Sustainable Buildings: A Systematic Review with Taxonomy, Challenges, Motivations, Methodological Aspects, Recommendations, and Pathways for Future Research. *Energy Strat. Rev.* **2023**, *45*, 101013. [CrossRef]
- Losini, A.; Grillet, A.; Bellotto, M.; Woloszyn, M.; Dotelli, G. Natural additives and biopolymers for raw earth construction stabilization—A review. *Constr. Build. Mater.* **2021**, *304*, 124507. [CrossRef]
- Oskouei, A.V.; Afzali, M.; Madadipour, M. Experimental investigation on mud bricks reinforced with natural additives under compressive and tensile tests. *Constr. Build. Mater.* **2017**, *142*, 137–147. [CrossRef]

20. Araya-Letelier, G.; Antico, F.; Carrasco, M.; Rojas, P.; García-Herrera, C. Effectiveness of new natural fibers on damage-mechanical performance of mortar. *Constr. Build. Mater.* **2017**, *152*, 672–682. [[CrossRef](#)]
21. Mamun, A.; Rafii, M.Y.; Misran, A.B.; Berahim, Z.; Ahmad, Z.; Khan, M.H.; Oladosu, Y.; Arolu, F. Kenaf (*Hibiscus cannabinus* L.): A Promising Fiber Crop with Potential for Genetic Improvement Utilizing both Conventional and Molecular Approaches. *J. Nat. Fibers* **2023**, *20*, 2145410. [[CrossRef](#)]
22. Laborel-Préneron, A.; Aubert, J.E.; Magniont, C.; Tribout, C.; Bertron, A. Plant aggregates and fibers in earth construction materials: A review. *Constr. Build. Mater.* **2016**, *111*, 719–734. [[CrossRef](#)]
23. Parisi, F.; Asprone, D.; Fenu, L.; Prota, A. Experimental characterization of Italian composite adobe bricks reinforced with straw fibers. *Compos. Struct.* **2015**, *122*, 300–307. [[CrossRef](#)]
24. Giroudon, M.; Laborel-Préneron, A.; Aubert, J.-E.; Magniont, C. Comparison of barley and lavender straws as bioaggregates in earth bricks. *Constr. Build. Mater.* **2019**, *202*, 254–265. [[CrossRef](#)]
25. Jannat, N.; Hussien, A.; Abdullah, B.; Cotgrave, A. Application of agro and non-agro waste materials for unfired earth blocks construction: A review. *Constr. Build. Mater.* **2020**, *254*, 119346. [[CrossRef](#)]
26. Bruno, A.W.; Gallipoli, D.; Perlot, C.; Kallel, H. Thermal performance of fired and unfired earth bricks walls. *J. Build. Eng.* **2020**, *28*, 101017. [[CrossRef](#)]
27. Bogas, J.A.; Silva, M.; Gomes, M.D.G. Unstabilized and stabilized compressed earth blocks with partial incorporation of recycled aggregates. *Int. J. Arch. Herit.* **2018**, *13*, 569–584. [[CrossRef](#)]
28. Oti, J.; Kinuthia, J.; Bai, J. Design thermal values for unfired clay bricks. *Mater. Des.* **2010**, *31*, 104–112. [[CrossRef](#)]
29. Benkhadda, N.; Khaldoun, A. *Effective Unfired Clay Bricks with Natural Additives*; School of Science & Engineering Al Akhawayn University: Ifrane, Morocco, 2019.
30. Ionescu, G.-L. Passive House. *J. Appl. Eng. Sci.* **2017**, *7*, 23–27. [[CrossRef](#)]
31. Fuentes, C.A.; Tran, L.Q.N.; Dupont-Gillain, C.; Van Vuure, A.W.; Verpoest, I. Interfaces in Natural Fibre Composites: Effect of Surface Energy and Physical Adhesion. *J. Biobased Mater. Bioenergy* **2012**, *6*, 456–462. [[CrossRef](#)]
32. Strazzeri, V.; Karrech, A. Energy and thermal performance of a typical rammed earth residential building in Western Australia. *Energy Build.* **2022**, *260*, 111901. [[CrossRef](#)]
33. Rivera-Gómez, C.; Galán-Marín, C.; Bradley, F. Analysis of the Influence of the Fiber Type in Polymer Matrix/Fiber Bond Using Natural Organic Polymer Stabilizer. *Polymers* **2014**, *6*, 977–994. [[CrossRef](#)]
34. Hamard, E.; Morel, J.-C.; Salgado, F.; Marcom, A.; Meunier, N. A procedure to assess the suitability of plaster to protect vernacular earthen architecture. *J. Cult. Herit.* **2013**, *14*, 109–115. [[CrossRef](#)]
35. Belfiore, C.M.; Amato, C.; Pezzino, A.; Viccaro, M. An end of waste alternative for volcanic ash: A resource in the manufacture of ceramic tiles. *Constr. Build. Mater.* **2020**, *263*, 120118. [[CrossRef](#)]
36. Aymerich, F.; Fenu, L.; Meloni, P. Effect of reinforcing wool fibres on fracture and energy absorption properties of an earthen material. *Constr. Build. Mater.* **2012**, *27*, 66–72. [[CrossRef](#)]
37. *EN 1015-11:2019*; Methods of test for mortar for masonry - Part 11: Determination of flexural and compressive strength of hardened mortar. EUROPEAN COMMITTEE FOR STANDARDIZATION, CEN-CENELEC Management Centre: Brussels, Belgium, 2019.
38. Parlato, M.C.M.; Rivera-Gómez, C.; Porto, S.M.C. Reuse of livestock waste for the reinforcement of rammed-earth materials: Investigation on mechanical performances. *J. Agric. Eng.* **2023**. [[CrossRef](#)]
39. Parlato, M.C.; Porto, S.M.; Valenti, F. Assessment of sheep wool waste as new resource for green building elements. *Build. Environ.* **2022**, *225*, 109596. [[CrossRef](#)]
40. Parlato, M.; Cuomo, M.; Porto, S. Natural fibers reinforcement for earthen building components: Mechanical performances of a low quality sheep wool (“Valle del Belice” sheep). *Constr. Build. Mater.* **2022**, *326*, 126855. [[CrossRef](#)]
41. *ASTM D5334-14*; Standard Test Method for Determination of Thermal Conductivity of Soil and Soft Rock by Thermal Needle Probe Procedure. American National Standards Institute (ANSI): Washington, DC, USA, 2000.
42. Carslaw, H.S.; Jaeger, J.C. *Conduction of Heat in Solids*, 2nd ed.; Oxford University Press: Oxford, UK, 1959; p. 38.
43. Rózański, A.; Sobótka, M. On the Interpretation of the Needle Probe Test Results: Thermal Conductivity Measurement of Clayey SOILS. *Stud. Geotech. Mech.* **2014**, *35*, 195–207. [[CrossRef](#)]
44. Arrigoni, A.; Grillet, A.-C.; Pelosato, R.; Dotelli, G.; Beckett, C.T.; Woloszyn, M.; Ciancio, D. Reduction of rammed earth’s hygroscopic performance under stabilisation: An experimental investigation. *Build. Environ.* **2017**, *115*, 358–367. [[CrossRef](#)]
45. Zach, J.; Hroudova, J.; Brozovsky, J. Study of Hydrothermal Behavior of Thermal Insulating Materials Based On Natural Fibers. *Int. J. Civ. Environ. Struct. Constr. Archit. Eng.* **2014**, *8*, 995–998.
46. Jerman, M.; Palomar, I.; Kočí, V.; Černý, R. Thermal and hygric properties of biomaterials suitable for interior thermal insulation systems in historical and traditional buildings. *Build. Environ.* **2019**, *154*, 81–88. [[CrossRef](#)]
47. Huson, M.G.; Cloutier, M.C. 3—Properties of wool. In *Handbook of Properties of Textile and Technical Fibres*, 2nd ed.; Bunsell, A.R., Ed.; Woodhead Publishing: Cambridge, UK, 2018; pp. 59–103. [[CrossRef](#)]
48. Rebolledo, P.; Cloutier, A.; Yemele, M.-C. Effect of Density and Fiber Size on Porosity and Thermal Conductivity of Fiberboard Mats. *Fibers* **2018**, *6*, 81. [[CrossRef](#)]
49. Nocera, F.; Caponetto, R.; Giuffrida, G.; Detommaso, M. Energetic Retrofit Strategies for Traditional Sicilian Wine Cellars: A Case Study. *Energies* **2020**, *13*, 3237. [[CrossRef](#)]

50. Giuffrida, G.; DeTommaso, M.; Nocera, F.; Caponetto, R. Design Optimisation Strategies for Solid Rammed Earth Walls in Mediterranean Climates. *Energies* **2021**, *14*, 325. [[CrossRef](#)]
51. Rivera-Gómez, C.; Galán-Marín, C.; López-Cabeza, V.P.; Diz-Mellado, E. Sample key features affecting mechanical, acoustic and thermal properties of a natural-stabilised earthen material. *Constr. Build. Mater.* **2021**, *271*, 121569. [[CrossRef](#)]

Disclaimer/Publisher's Note: The statements, opinions and data contained in all publications are solely those of the individual author(s) and contributor(s) and not of MDPI and/or the editor(s). MDPI and/or the editor(s) disclaim responsibility for any injury to people or property resulting from any ideas, methods, instructions or products referred to in the content.